Published in final edited form as:
Cell Rep. 2015 January 6; 10(1): 62–74. doi:10.1016/j.celrep.2014.12.011.

An Estrogen-Responsive Module in the Ventromedial Hypothalamus Selectively Drives Sex-Specific Activity in Females

Stephanie M. Correa[1], **David W. Newstrom**[1], **James P. Warne**[2], **Pierre Flandin**[3], **Clement C. Cheung**[1,4], **Alexander T. Lin-Moore**[1], **Andrew A. Pierce**[5], **Allison W. Xu**[2,6], **John L. Rubenstein**[3,*], and **Holly A. Ingraham**[1,2,*]

[1]Department of Cellular and Molecular Pharmacology, University of California, San Francisco, San Francisco, CA 94143

[2]Diabetes Center, University of California, San Francisco, San Francisco, CA 94143

[3]Department of Psychiatry, University of California San Francisco, San Francisco, CA 94143

[4]Department of Pediatrics, University of California San Francisco, San Francisco, CA 94143

[5]Liver Center, University of California San Francisco, San Francisco, CA 94143

[6]Department of Anatomy, University of California San Francisco, San Francisco, CA 94143

Abstract

Estrogen-receptor alpha (ERα) neurons in the ventrolateral region of the ventromedial hypothalamus (VMH_{VL}) control an array of sex-specific responses to maximize reproductive success. In females, these VMH_{VL} neurons are believed to coordinate metabolism and reproduction. However, it remains unknown whether specific neuronal populations control distinct components of this physiological repertoire. Here, we identify a subset of ERα VMH_{VL} neurons that promotes hormone-dependent female locomotion. Activating *Nkx2-1*-expressing VMH_{VL} neurons via pharmacogenetics elicits a female-specific burst of spontaneous movement, which requires ERα and *Tac1* signaling. Disrupting development of *Nkx2-1*$^{+}$ VMH_{VL} neurons results in female-specific obesity, inactivity, and loss of VMH_{VL} neurons co-expressing ERα and *Tac1*. Unexpectedly, two responses controlled by ERα neurons, fertility and brown adipose tissue thermogenesis, are unaffected. We conclude that a dedicated subset of VMH_{VL} neurons marked

*Correspondence to: john.rubenstein@ucsf.edu and holly.ingraham@ucsf.edu.

Author Contributions

SMC, JPW, and HI designed the pharmacogenetics experiments, performed by SMC, JPW, and ATLM. HI and JLR designed and provided intellectual guidance on the *Nkx2-1*$^{f/f}$*/Sf1Cre* experiment. SMC, DWM, PF, CCC, ATLM and AAP analyzed the *Nkx2-1*$^{f/f}$*/Sf1Cre* phenotype. SMC and HI wrote the manuscript with input from JLR, JPW, CCC, AWX, DWN and ATLM.

The authors declare no competing interests.

by ERα, NKX2-1, and *Tac1* regulates estrogen-dependent fluctuations in physical activity and constitutes one of several neuroendocrine modules that drive sex-specific responses.

Introduction

Investment in reproduction is vastly different between female and male mammals. In females, the tradeoff between energy storage versus energy usage during pregnancy/lactation dramatically affects reproductive outcomes. The integration of reproduction and metabolism in females is mediated in large part by the actions of ovarian hormones in the brain. Indeed, estrogen-responsive neurons in the hypothalamus are believed to regulate sexual receptivity, fertility, food intake, and two components of energy expenditure: thermogenesis and physical activity in females (Musatov et al., 2006; Musatov et al., 2007; Xu et al., 2011). Dissecting the neuronal populations and hormonal pathways that drive these distinct physiological responses is critical for understanding how reproduction and metabolism are integrated to maximize reproductive success.

The ventrolateral region of the female ventromedial hypothalamic nucleus (VMH_{VL}) regulates fertility, sexual receptivity and energy expenditure, as shown by electrolytic and genetic lesions (King and Frohman, 1985; Pfaff and Sakuma, 1979; Yang et al., 2013). The VMH_{VL} develops from the Steroidogenic factor 1 (SF-1, *Nr5a1*) lineage but does not express SF-1 by birth (Cheung et al., 2012). Eliminating SF-1 in the brain disrupts the normal organization of the VMH, including the VMH_{VL}, and leads to female but not male infertility (Kim et al., 2010). Within the VMH, it is the VMH_{VL} that exhibits marked sex differences with respect to size (Dorner and Staudt, 1969; Madeira et al., 2001), synaptic organization (Griffin and Flanagan-Cato, 2009; Larriva-Sahd et al., 1995), and hormone responsiveness (MacLusky and McEwen, 1980; Pfaff and Keiner, 1973). Estrogen receptor alpha (ERα) is highly enriched in the adult female VMH_{VL} with much lower expression detected in adult male VMH_{VL} (Koch, 1990). Of note, expression of the other two known estrogen receptors, estrogen receptor beta (ERβ) (Zuloaga et al., 2014) and G protein-coupled estrogen receptor 1 (GPER, GPR30) (Brailoiu et al., 2007), is sparse or undetectable in the adult VMH_{VL}. In the rodent VMH, ERα plays an important role in female reproduction and sexual receptivity as evidenced in the global (Lubahn et al., 1993) and conditional knockouts (Xu et al., 2011), as well as in shRNA-knockdown (Musatov et al., 2006) studies.

Estrogen signaling via ERα in the VMH_{VL} is also critical for energy balance. ShRNA knockdown of ERα in the VMH increases food intake and decreases diet-induced thermogenesis and physical activity, resulting in obesity (Musatov et al., 2007). Conditional knockout of ERα in the VMH using *Sf1Cre* also lowers brown adipose tissue (BAT) thermogenesis in female mice, and yields a mild transient weight gain in females due to increased size of gonadal fat pads (Xu et al., 2011). Although these studies are the best to date in dissecting the role of ERα in the VMH, results obtained from $Esr1^{f/f}/Sf1Cre$ females, results are confounded by the loss of ERα in peripheral endocrine organs, including the ovary.

Despite the clear importance of the VMH_{VL} in female physiology, it remains unclear whether shared or distinct estrogen-responsive neurons regulate reproduction and energy balance. Here, using complementary gain- and loss-of-function strategies, we asked if fertility and two different metabolic responses, BAT thermogenesis and locomotion, are regulated by identical or different VMH_{VL} neurons. To do this, the enriched expression of the NK2 homeobox transcription factor 1 (*Nkx2-1*, *Ttf1*) (Kurrasch et al., 2007; Tran et al., 2003) in the VMH_{VL} was leveraged to activate these neurons using pharmacogenetics. Conversely, conditional knockout of *Nkx2-1* was used to disrupt normal development of VMH_{VL} neurons. Together, these two approaches show that a subset of VMH_{VL} neurons promote spontaneous physical activity in female but not male mice, without affecting reproduction. This locomotor response is sex hormone-dependent and requires intact estrogen signaling via ERα as well as the neuropeptide-encoding gene Tachykinin 1 (*Tac1*). Our data imply that females utilize separate hormone-responsive modules in the VMH_{VL} to optimize and coordinate reproduction and metabolism.

Results

Activating Nkx2-1 VMH_{VL} neurons increases activity in females

The postnatal VMH_{VL} is a neuronal cluster that is marked by ERα and NKX2-1 (Fig. 1A). By embryonic day (E) 11.5, VMH progenitors including those that will populate the VMH_{VL} express NKX2-1 as well as SF-1 (Fig. 1B, C). Prior to birth, the VMH_{VL} no longer expresses SF-1 and becomes a molecularly distinct VMH subregion (Cheung et al., 2012), as evidenced here by the complementary expression of SF-1 and NKX2-1 at postnatal day (P) 0 (Fig. 1D). The enriched expression of NKX2-1 in the VMH_{VL} (Fig. S1) permitted us to examine sex-specific metabolic responses associated with VMH_{VL} neurons. NKX2-1 neurons in the VMH_{VL} were artificially activated using designer receptors exclusively activated by designer drugs (DREADDs) in *Nkx2-1-Cre* mice. Stereotaxic delivery of the *Cre*-dependent AAV-hM3Dq-mCherry DREADD was confirmed by mCherry expression in the VMH_{VL} of *Nkx2-1Cre* male and female mice (Fig. 1E, F). Little or no mCherry expression was observed in the VMH_{VL} of virus-injected adult *Sf1Cre* female mice (Fig. 1E), consistent with the idea that most VMH_{VL} neurons express SF-1 only during early development. mCherry was not detected in wild-type mice (Fig. 1F, S2A).

Activating *Nkx2-1*$^{+}$ VMH_{VL} neurons using DREADDs elicits marked sex differences in movement (Fig. 1G). Specifically, administering the synthetic ligand clozapine-N4-oxide (CNO) during the inactive light phase elicits rapid and sustained increases in total, ambulatory, and vertical movements only in *Nkx2-1Cre* females (Fig. 1G, S3, Movie S1). On average, CNO-induced responses persist for 2 h, reaching a maximal response within the first hour post-injection. CNO injections to *Nkx2-1Cre* females also increase oxygen consumption (VO_2) and heat generation (Fig. 1G, S3). Notably, CNO given 24 or 48 h apart is equally effective at increasing locomotion (Fig. S2D). In striking contrast, *Nkx2-1Cre* males, *Sf1Cre* females, and wild-type mice failed to exhibit significant DREADD-induced changes in all aspects of movement (Fig. 1G, S3). However, CNO elicits a modest VO_2 increase in *Nkx2-1Cre* males, which could be attributed to small insignificant increases in male movement and heat generation (Fig. 1G, S3). CNO also failed to elicit an increase in

food intake in either sex (Fig. S3) in contrast to hyperphagia observed after DREADD activation of Agouti-related protein (*Agrp*)-expressing neurons in the arcuate nucleus (ARC) (Krashes et al., 2011). Expression of cFOS confirmed VMH_{VL} neuron activation by CNO in both *Nkx2-1Cre* males and females (Fig. 2A). Further, while a correlation between the magnitude of the response and the intensity or spread of DREADD expression might be expected (Lee et al., 2014; Silva et al., 2013), this is not the case in our study; CNO-induced activity is observed in females with unilateral or modest mCherry expression in the VMH_{VL} (Fig. S2A, C). We also found that DREADD activation of *Nkx2-1* neurons in the lateral hypothalamus (LH), which has been linked to activity and wakefulness (Sasaki et al., 2011), does not significantly affect oxygen consumption or total movement (refer to Fig. S7C, D). Taken together these data establish that activating *Nkx2-1* neurons in the VMH_{VL} drives spontaneous movement primarily in females (Fig. 2B).

Developmental Nkx2-1 ablation results in female-specific obesity due to decreased activity

To ask how disrupting the development of the VMH_{VL} might impact reproduction and metabolism in females, the *Sf1Cre* driver was used to conditionally knock out *Nkx2-1* in the VMH (Fig. 3A). To begin to probe *Nkx2-1* function, we used the VMH-specific *Sf1Cre* driver that will eliminate Nkx2-1 during development beginning at E9. SF-1 expression in the VMH begins at the onset of neurogenesis and overlaps with NKX2-1 at E13.5, particularly in the periventricular layer (Fig. 1B). In P0 *Nkx2-1$^{f/f}$/Sf1Cre* mice, NKX2-1 expression is extinguished in the VMH_{VL} region, but continues to be expressed in the ventricular zone, the ARC and the dorsal medial hypothalamus (DMH) (Fig. 3A). Further, NKX2-1 is deleted only in the VMH, consistent with the non-overlapping expression patterns of NKX2-1 and SF-1 outside of the VMH (Fig. S4A, B). The VMH of *Nkx2-1$^{f/f}$/Sf1Cre* mice appears grossly normal at E13.5, as judged by the expression of numerous well-defined (Kurrasch et al., 2007) VMH-enriched markers (Fig. 3B). These findings suggest that ablating *Nkx2-1* in postmitotic VMH neurons after E10.5 (Cheung et al., 2012) does not disrupt the overall patterning of the VMH.

Beginning at 8 weeks of age, *Nkx2-1$^{f/f}$/Sf1Cre* females are significantly heavier than their *Nkx2-1$^{f/f}$* littermates (Fig. 4A, B). This metabolic phenotype reflects the VMH-specific loss of *Nkx2-1* (Fig. S4A), and persists throughout adulthood. Unlike many mouse models of obesity, this weight increase is observed when fed a breeder chow diet (21.6% kcal from fat). In contrast, *Nkx2-1$^{f/f}$/Sf1Cre* male mice do not show a measureable body weight phenotype (Fig. 4B), and only show a modest weight gain, exceeding that of control littermates beginning at 4 weeks of high fat diet (HFD, 60% kcal fat) feeding (Fig. S4C). *Nkx2-1$^{f/f}$/Sf1Cre* females are heavier because of increased fat (~10g) and lean (~5g) mass with no changes in body length or skeletal composition observed (Fig. 4C, D and S4E). Accordingly, all white adipose depots (Fig. 4E, F, and S4E) and plasma leptin concentration (Fig. 4E) are significantly greater in *Nkx2-1$^{f/f}$/Sf1Cre* females. However, no changes in BAT depot weight or thermogenic gene expression are detected in *Nkx2-1$^{f/f}$/Sf1Cre* females (Fig. 4E–G), demonstrating that BAT thermogenesis is normal in these obese female mice. The metabolic phenotype in *Nkx2-1$^{f/f}$/Sf1Cre* females is also unexpectedly uncoupled from reproduction. Indeed, litter size, days between litters, plasma estradiol concentration, and ovarian histology are unaltered in *Nkx2-1$^{f/f}$/Sf1Cre* females (Fig. 4H). Despite the

established role of the VMH_{VL} in promoting social behaviors (Lee et al., 2014; Lin et al., 2011; Silva et al., 2013; Yang et al., 2013), we find that *Nkx2-1*$^{f/f}$*/Sf1Cre* males exhibit wild-type levels of aggression in resident-intruder trials (Fig. S5A) and *Nkx2-1*$^{f/f}$*/Sf1Cre* mice of both sexes exhibit normal levels of anxiety in an open field (Fig. S5B, D). Thus, the loss of *Nkx2-1* in the VMH_{VL} appears to selectively disrupt energy homeostasis in females.

To further define the underlying cause of the obesity phenotype of *Nkx2-1*$^{f/f}$*/Sf1Cre* females, energy intake and expenditure were assessed. Food intake is unchanged in singly housed *Nkx2-1*$^{f/f}$*/Sf1Cre* females when compared to their weight-matched wild-type littermates (Fig. 5A). However VO_2, heat generated, and physical activity are all significantly lower in 22-week old *Nkx2-1*$^{f/f}$*/Sf1Cre* females (Fig. 5B, C). Specifically, *Nkx2-1*$^{f/f}$*/Sf1Cre* females exhibit lower VO_2 (mL/h) for a given lean mass and lower heat generation (kcal/h) for a given total body mass during the light and dark phases (Fig. 5B). This apparent decrease in energy expenditure is associated with less movement in *Nkx2-1*$^{f/f}$*/Sf1Cre* females during the light and dark cycles (Fig. 5C). *Nkx2-1*$^{f/f}$*/Sf1Cre* females also exhibit lower running wheel activity at 7 weeks of age, before any significant weight gain (Fig. 5D). Taken together, these data indicate that *Nkx2-1* ablation in the VMH leads to decreased locomotion and consequent obesity in females, while leaving BAT thermogenesis intact.

Obese Nkx2-1$^{f/f}$/Sf1Cre females have fewer estrogen-responsive Tac1 VMH_{VL} neurons

Next, we asked if estrogen signaling is altered in the VMH_{VL} of *Nkx2-1*$^{f/f}$*/Sf1Cre* females. ERα and NKX2-1 are coexpressed in a subset of VMH_{VL} neurons (Fig. 6A,B). In *Nkx2-1*$^{f/f}$*/Sf1Cre* females, the number of ERα-positive VMH_{VL} neurons is reduced by 26% (Fig. 6A, B) consistent with a reduction in *Esr1* transcripts (Fig. 6D, F). Similarly, we observe 25% fewer VMH_{VL} neurons, as judged by *Sf1Cre* lineage tracing (Fig 6C). Moreover, BrdU birth-dating studies show that the total number of VMH_{VL} neurons born at E11.5 (Ishii and Bouret, 2012; Tran et al., 2003) is 26% lower (Fig. S6A, B). Cell death is not a significant contributing factor in reducing VMH_{VL} neuron number, as no activated Caspase-3 is detected at E11.5, E13.5, E15.5 or E17.5 in the *Nkx2-1*$^{f/f}$*/Sf1Cre* female VMH (data not shown). Taken together, these data imply that a subset of ERα-expressing VMH_{VL} neurons fail to be born during development resulting in a smaller VMH_{VL}. Thus the VMH of *Nkx2-1*$^{f/f}$*/Sf1Cre* mice is grossly normal but missing approximately 25% of ERα-expressing VMH_{VL} neurons.

Transcriptional profiling was used to further define the identity of the neurons that are absent in the VMH_{VL} of *Nkx2-1*$^{f/f}$*/Sf1Cre* females. Consistent with our histological studies, only a few transcripts were altered in the *Nkx2-1*$^{f/f}$*/Sf1Cre* female VMH, including *Tachykinin 1 (Tac1), Galanin (Gal),* and *Neuromedin U (Nmu)* (Fig. 6D). Similar to *Esr1*, *Tac1* also is enriched in the female VMH_{VL} and colocalizes with ERα (Fig. 6E, F), as shown previously in rats (Dornan et al., 1990). Based on overlapping expression patterns, ERα, *Tac1*, and NKX2-1 appear to mark a subpopulation of VMH_{VL} neurons that is ablated in *Nkx2-1*$^{f/f}$*/Sf1Cre* females. Reduced *Tac1* and ERα in *Nkx2-1*$^{f/f}$*/Sf1Cre* females are accompanied by the presence of scattered VMH_{VL} neurons expressing *Gal* and *Gad67* (Fig. S5F). Both of these transcripts mark inhibitory neurons, which are normally excluded from the VMH (Dellovade et al., 2000). Increased ectopic expression of *Gal* and *Gad67* is

accompanied by an increase in non-SF-1 lineage, NeuN-positive neurons in the VMH_{VL} (Fig. S6C). This observation is consistent with the notion that the VMH_{VL} in *Nkx2-1*$^{f/f}$*/Sf1Cre* females is infiltrated by neurons from surrounding regions, rather than the switching of cell fates. Similar to females, the VMH_{VL} of *Nkx2-1*$^{f/f}$*/Sf1Cre* males is smaller by neuron number, and also exhibits ectopic expression of *Gal* and *Gad67* (Fig. S5C, F), suggesting that increased inhibitory tone cannot explain the female-specific inactivity and obesity phenotype.

Taken together, these data imply that a subpopulation of NKX2-1^{+} VMH_{VL} neurons co-expressing ERα and *Tac1* is enriched in females compared to males, and is largely absent in *Nkx2-1*$^{f/f}$*/Sf1Cre* females (Fig. 6F). This is in sharp contrast to eliminating ERα using *Sf1Cre* (*Esr1*$^{f/f}$*/Sf1Cre*), which results in normal *Nkx2-1, Tac1* and *Gal* expression (Fig. S6D, E), and importantly normal VMH_{VL} neuron number (Xu et al., 2011). Thus, we posit that the pronounced metabolic deficits exhibited by *Nkx2-1*$^{f/f}$*/Sf1Cre* females arise not only from reduced ERα signaling but also the developmental loss of a subset of sexually dimorphic VMH_{VL} neurons that express ERα, *Tac1*, and NKX2-1.

Physical activity is modulated by ERα and Tac1

To test whether *Tac1* and ERα-mediated estrogen signaling modulate female activity, we activated *Nkx2-1* neurons using *Cre*-dependent hM3Dq DREADDs in four different mouse models: 1) sham-operated-*Nkx2-1Cre*, 2) OVX-*Nkx2-1Cre*, 3) *Esr1*$^{f/f}$*/Nkx2-1Cre* and 4) *Tac1*$^{-/-}$*/Nkx2-1Cre* mice. In *Esr1*$^{f/f}$*/Nkx2-1Cre* mice, ERα is eliminated throughout the mediobasal hypothalamus (Fig. 7A) and in *Tac1*$^{-/-}$*/Nkx2-1Cre* mice, *Tac1* is eliminated globally (Fig. 7B). For these two genetic mouse models, we note that ERα and *Tac1* are eliminated independently. Targeting of DREADDs to the VMH_{VL} was confirmed by mCherry (Fig. S7A) and activation by CNO verified by cFOS (Fig. 7D, E). Of these four experimental conditions, sham-operated *Nkx2-1Cre* females showed the most robust locomotion responses to CNO, while significant but blunted responses were observed in *Tac1*$^{-/-}$*/Nkx2-1Cre* females (Fig. 7C, F). Loss of estrogen signaling in OVX or *Esr1*$^{f/f}$*/Nkx2-1Cre* females significantly reduced DREADD-induced locomotion (Fig. 7F). Similar trends are observed for VO_2 (Fig. S7B). Overall these results indicate that physical activity in *Nkx2-1* VMH_{VL} neurons is modulated by estrogen signaling and to a lesser extent by *Tac1* function.

Discussion

Here, we establish that estrogen-responsive, NKX2-1- and *Tac1*-expressing VMH_{VL} neurons are essential for normal physical activity in females. Activating *Nkx2-1*$^{+}$ VMH_{VL} neurons increases physical activity in female, but not male mice; this sex difference in DREADD-induced locomotion depends on estrogen, ERα, NKX2-1, and *Tac1*. Ablating this VMH_{VL} subpopulation in an *Nkx2-1*$^{f/f}$*/Sf1Cre* mouse model results in a sex-specific decrease in spontaneous physical activity without affecting BAT thermogenesis or fertility. Thus, while different facets of reproduction and metabolism are tightly coupled and phased to fluctuating ovarian hormone levels (Brobeck et al., 1947; Slonaker, 1925), results reported here clearly dissociate the metabolic and reproductive roles of ERα signaling in the

female VMH_{VL}. Taken together, these studies imply that $ER\alpha^{+}$ neurons can be divided into functionally distinct subpopulations that independently regulate the sex-specific behavioral and physiological functions ascribed to the VMH_{VL}.

Partitioning ERα VMH_{VL} Neurons Into Functionally Distinct Subpopulations

Genetic manipulations affecting the development and hormone signaling pathways of the VMH_{VL} are beginning to reveal the functional and molecular complexity of this VMH subregion. While NKX2-1 is required for patterning the rostroventral hypothalamus (Kimura et al., 1996; Marin et al., 2002; Shimamura and Rubenstein, 1997), ablation of *Nkx2-1* using *Sf1Cre* occurs late enough in development to leave the VMH largely intact; a similar result is observed when *Nkx2-1* is ablated in differentiated neurons using *SynapsinCre* (Mastronardi et al., 2006). Importantly, in the *Nkx2-1*$^{f/f}$*/Sf1Cre* mouse model, *Nkx2-1* remains intact both in other hypothalamic nuclei and in peripheral endocrine tissues. Consistent with earlier developmental studies of the VMH (Ishii and Bouret, 2012; Tran et al., 2003), our BrdU birth-dating analyses indicate that the earliest born neurons to populate and migrate to the VMH_{VL} fail to be born in embryonic *Nkx2-1*$^{f/f}$*/Sf1Cre* females. As a consequence, in adult females, estrogen signaling and other potential neuromodulators (*Tac1*) are diminished, leading to obesity.

The striking phenotypic differences in reproduction and metabolism observed between *Nkx2-1*$^{f/f}$*/Sf1Cre* and *Esr1*$^{f/f}$*/Sf1Cre* mouse models are instructive for dissecting out the complex and coordinated metabolic and reproductive functions of the VMH_{VL} in females. In both models, the same *Sf1Cre* driver was used to target two functionally distinct VMH_{VL} markers; NKX2-1 acts primarily as a developmental regulator, whereas ERα mediates estrogen signaling. Losing a subset of ERα neurons in *Nkx2-1*$^{f/f}$*/Sf1Cre* females results in inactivity and obesity while fertility and BAT thermogenesis are left intact. By contrast, in *Esr1*$^{f/f}$*/Sf1Cre* females, ablating nearly all ERα in the VMH_{VL} without neuronal loss significantly impairs BAT thermogenesis and fertility with a modest and transient increase in body weight (Xu et al., 2011). It is possible that BAT thermogenesis (and fertility) is maintained in *Nkx2-1*$^{f/f}$*/Sf1Cre*, but not in *Esr1*$^{f/f}$*/Sf1Cre*, females because of sufficient estrogen signaling, consistent with the hypothalamic actions of estrogen on BAT thermogenesis (Martinez de Morentin et al., 2014). On the other hand, physical activity is reduced in *Nkx2-1*$^{f/f}$*/Sf1Cre* but not *Esr1*$^{f/f}$*/Sf1Cre* females. We attribute this phenotype in *Nkx2-1*$^{f/f}$*/Sf1Cre* females to the developmental loss of a subset of ERα VMH_{VL} neurons rather than simply reflecting changes in the levels of ERα. Taken together, these data also suggest that distinct subpopulations of estrogen-responsive neurons in the VMH_{VL} parse out the array of physiological and behavioral responses associated with this hypothalamic subregion.

For this subset of ERα, *Tac1* VMH_{VL} neurons, it will be important to define which neuromodulators and what projections drive spontaneous activity in females. In this regard, neuropeptide signaling encoded by *Tac1* is likely to participate in the modulation of female-specific movement. Indeed, *Tac1* is enriched in the female VMH_{VL}, as previously reported for rats (Dornan et al., 1990), it is lower in *Nkx2-1*$^{f/f}$*/Sf1Cre* but not in *Esr1*$^{f/f}$*/Sf1Cre* females, and is required for the full increase in DREADD-induced locomotion. Global

knockouts of *Tac1* or the SP receptor (NK-1) exhibit improved glucose homeostasis (Karagiannides et al., 2011a) and resistance to diet-induced obesity (Karagiannides et al., 2011b); unfortunately both studies only report data from male mice. ERα$^+$, *Tac1*$^+$ VMH neurons may project to MPOA neurons, which have been linked to estrogen-induced running in rats (Fahrbach et al., 1985; Spiteri et al., 2012). Other VMH projections relevant to locomotion might include those to the subthalamic and mesencephalic locomotor regions (SLR and MLR)(Cheung et al., 2012), areas that when activated increase controlled movement in rats (Skinner and Garcia-Rill, 1984) or when lesioned in humans lead to deficits in locomotion (Hathout and Bhidayasiri, 2005). Interestingly, pharmacologic activation of the VMH induces wheel running and neural activity in the SLR (Narita et al., 2002). Future genetic tracing using reagents that allow us to precisely map projections from VMH_{VL} neuronal subpopulations will address how this cluster of neurons controls locomotion in females.

Sex-Differences in Hormone-Dependent Behaviors Mediated by the VMH_{VL}

Loss- and gain-of-function analyses presented in this study reveal that regulation of spontaneous movement by NKX2-1 VMH_{VL} neurons is largely sex-specific. Male mice fail to show the same DREADD-induced responses with respect to locomotion, but do exhibit a modest increase in oxygen consumption. Although increased oxygen consumption was not associated with higher locomotion or heat generation, we cannot exclude the possibility that VMH_{VL} neurons play a minor role in male locomotion. Indeed, pharmacologic activation in the VMH_{VL} induces running in male rats (Narita 1993). *Nkx2-1*$^{f/f}$*/Sf1Cre* males exhibit the same loss of ERα, *Tac1* and NKX2-1 neurons, but maintain normal body weights on standard chow and a slightly elevated body weight when fed a HFD. These data indicate that ERα, *Tac1* and NKX2-1 VMH_{VL} neurons function primarily in females and play only a minor role in male energy expenditure. Whether female-enriched expression of ERα and *Tac1* is sufficient to drive sex-differences in locomotion and body weight remains to be firmly established.

While these VMH_{VL} neurons have a modest effect on energy balance in males, others have shown that ERα- and progesterone receptor (PR)-positive VMH_{VL} neurons are critical for mating and aggressive behaviors in males (Lee et al., 2014; Lin et al., 2011; Yang et al., 2013). Even though activating *Nkx2-1* neurons in the VMH_{VL} via DREADDs should increase a wide variety of behaviors associated with VMH_{VL}, including male aggression, *Nkx2-1*$^{f/f}$*/Sf1Cre* males exhibit normal aggression, fertility and anxiety. This leads us to speculate that regulation of social behaviors in male mice must involve a different subset(s) of ERα$^+$ VMH_{VL} neurons distinct from the ERα, *Tac1* and NKX2-1 neurons lost in *Nkx2-1*$^{f/f}$*/Sf1Cre* males. We also note that within the VMH_{VL}, the DREADD-induced activation of locomotion in females appears much more sensitive when compared to DREADD- or ChR-induced activation of behaviors in males (Lee et al., 2014; Silva et al., 2013). Indeed, increased movement is observed in females even after unilateral or limited infection of DREADDs into VMH_{VL} neurons. It will be of interest to determine whether this apparent sex difference in sensitivity reflects the use of DREADDs versus ChRs, or reflects inherent differences in social (contextual) versus spontaneous behaviors.

The ability to blunt DREADD-induced movement by genetic deletion of ERα, as shown here, establishes that ERα signaling is the main mediator of hormone-induced movement, as previously reported for female sexual behavior (Lubahn et al., 1993; Musatov et al., 2006). Hormone dependency has yet to be shown for experimentally induced male behaviors, including social fear, mating, and aggression (Lee et al., 2014; Silva et al., 2013). It is also unclear how estrogen, whether signaling through genomic or non-classical rapid mechanisms (Frank et al., 2014), modulates DREADD responses. Estrogens via ERα might directly modulate Gq-mediated signaling, as suggested previously (Farrell and Roth, 2013; Mermelstein, 2009), or alternatively, the loss of ERα signaling during development might permanently alter neuronal excitability or circuitry to and from the VMH_{VL}. Surprisingly, there was little variation in DREADD responses in cycling females suggesting that DREADD-induced locomotion is insensitive to normal fluctuations in estrogen. It is only after eliminating all gonadal hormones or all ERα signaling that we are able to detect the impact of estrogen signaling on DREADD-induced locomotion. Our findings are consistent with little to no effect of the estrous cycle on locomotion in mice (Kopp et al., 2006), implying that the influence of the estrous cycle on physical activity is far stronger in rats than in mice. Nonetheless, our data demonstrate that the absence of sex hormone signaling blunts sex-specific DREADD responses, a feature that has yet to be established for ChRs.

In summary, we identify a subset of VMH_{VL} neurons that constitute part of a previously undefined sex-specific locomotor circuit that is used in females to promote hormone-responsive movement and maintain metabolic fitness. Increased movement prior to ovulation (high estrogen) in non-primate mammals (Brobeck et al., 1947; Kopp et al., 2006; Saint-Dizier and Chastant-Maillard, 2012; Slonaker, 1925) might provide a reproductive advantage during periods of maximal sexual receptivity, as previously hypothesized (Morgan and Pfaff, 2002). Hence, the tight linkage between energy expenditure and fertility may result from the parallel actions of estrogens on functionally distinct estrogen-responsive modules that together maximize female reproductive success. Clearly, it now becomes important to understand how female VMH_{VL} functional modules acquire their sex-specific properties and how they interact to coordinate reproduction and metabolism. Ultimately, the existence of a similar estrogen-sensitive locomotion module in women could be relevant for understanding the metabolic consequences of menopause (Carr, 2003) and disease-associated ERα polymorphisms (Ghattas et al., 2013; Okura et al., 2003).

Experimental Procedures

Pharmacogenetics

The *Cre*-dependent AAV-hM3Dq-mCherry DREADD (UNC Vector Core) was injected bilaterally into anesthetized (100 mg/kg ketamine, 5 mg/kg xylazine, i.p.) adult mice (9–16 weeks old, coordinates: A-P: −1.56 mm from Bregma, lateral: +/−0.85 mm from Bregma, D-V: −5.8 mm from the skull). Buprenorphine (0.1 mg/kg i.p.) was provided for analgesia immediately after surgery and as required. After two-weeks of recovery and 41 h acclimation in metabolic chambers, mice received three daily intraperitoneal (IP) injections: two CNO (0.3 mg/kg) and one saline 3 h after the onset of the light phase. On the first two days, saline and CNO were administered in a randomized balanced design. On the third day,

all subjects received CNO, thus subjects received CNO injections either 24 h or 48 h apart. For OVX mice, OVX surgery and stereotaxic DREADD injection were performed in the same surgical sitting.

Metabolic Analyses

Comprehensive Laboratory Animal Monitoring Systems (CLAMS) measured O_2 consumption, CO_2 exhalation, total movement (total beam breaks, X and Y axes), ambulatory movement (adjacent beam breaks, X and Y axes) and rearing (total beam breaks, Z axis) at 14 minute intervals. Food intake was determined via CLAMS for DREADDs studies or in singly housed mice for *Nkx2-1*$^{f/f}$*/Sf1Cre* studies, carefully accounting for spillage. Mice were housed in CLAMS for 96 h, however the first 24–48 h (acclimation) were not included in the analyses. For DREADDs experiments, VO_2 measurements were standardized to lean mass. However, because each mouse served as its own control, the standardization does not affect the results. For *Nkx2-1*$^{f/f}$*/Sf1Cre* studies, ANCOVA was used to compare raw values for VO_2, heat generated and food intake between control and mutant mice. EchoMRI and DEXA were used to measure body composition. Except for OVX studies, all CLAMS analyses in females were performed in intact, cycling animals.

Expression profiling

Total RNA from microdissected VMH was isolated using the PureLink RNA kit (Invitrogen) and analyzed in quadruplicate using Mouse Ref8 v2.0 array chips (Illumina). P10 pups were used to avoid any effects of the estrous cycle on transcript abundance. Microarray data were normalized using quantile normalization, differential expression analysis was performed as previously described (Coppola, 2011), and significance threshold set at $p<0.005$. Raw and normalized data were deposited in GEO (GSE63656). For qPCR, RNA was DNase-treated, reverse transcribed with SuperScript III (Invitrogen), and amplified in triplicate using PerfeCta SYBR Green SuperMix (Quanta Biosciences). Cryosections (20μm) for immunohistochemistry (IHC) and RNA *in situ* hybridization (ISH) were collected from brains fixed in 4% paraformaldehyde. DIG-labeled riboprobes were transcribed from published plasmids except for *Nmu* (FL cDNA from Open Biosystems) and *Gal* for which cDNA (bases 34–614) was cloned into pCRII-TOPO (Invitrogen).

See Extended Experimental Procedures for mouse strains, histology, primer sequences, hormone measurements and statistical analyses.

Supplementary Material

Refer to Web version on PubMed Central for supplementary material.

Acknowledgements

We thank Drs. A. Basbaum, R. Blind, M. Dallman, Y.-H. Fu, C. Herber, A. Kreitzer, W. Krause, T. McMahon, C. Paillart, L. Ptacek, N. Shah, S. Silberberg, T. Tachibana, J. Tollkuhn, and L. Zhang for reagents and discussion, Fuyng Gao and Giovanni Coppola for assistance with microarray data analysis. This research was supported by grants to HAI (NIDDK R01DK063592, R01DK099722, UCSF Diabetes Family Fund, AHA Grant-in-Aid 13GRNT16120004), JLR (NIMH R01 MH081880, R37 MH049428), SMC (NIDDK K01DK098320, AHA Postdoctoral Fellowship 12POST10690005), CCC (NIDDK K08DK076721), AWX (NIDDK R01DK80427), and DWM (CIRM SFSU Bridges grant). We acknowledge the UCSF DERC (NIDDK P30 DK063720), Liver Center

(NIDDK P30 DK026743), Nikon Imaging Center, UCSF Neurobehavioral Core, Gladstone Institutes Histology Core, and UCLA Neuroscience Genomics Cores. We acknowledge the support of the UCLA NINDS Informatics Center for Neurogenetics and Neurogenomics (P30 NS062691).

References

Brailoiu E, Dun SL, Brailoiu GC, Mizuo K, Sklar LA, Oprea TI, Prossnitz ER, Dun NJ. Distribution and characterization of estrogen receptor G protein-coupled receptor 30 in the rat central nervous system. J Endocrinol. 2007; 193:311–321. [PubMed: 17470522]

Brobeck JR, Wheatland M, Strominger JL. Variations in regulation of energy exchange associated with estrus, diestrus and pseudopregnancy in rats. Endocrinology. 1947; 40:65–72. [PubMed: 20286603]

Carr MC. The emergence of the metabolic syndrome with menopause. J Clin Endocrinol Metab. 2003; 88:2404–2411. [PubMed: 12788835]

Cheung CC, Kurrasch DM, Liang JK, Ingraham HA. Genetic labeling of steroidogenic factor-1 (SF-1) neurons in mice reveals ventromedial nucleus of the hypothalamus (VMH) circuitry beginning at neurogenesis and development of a separate non-SF-1 neuronal cluster in the ventrolateral VMH. J Comp Neurol. 2012; 521:1268–1288. [PubMed: 22987798]

Coppola G. Designing, performing, and interpreting a microarray-based gene expression study. Methods Mol Biol. 2011; 793:417–439. [PubMed: 21913117]

Dellovade TL, Young M, Ross EP, Henderson R, Caron K, Parker K, Tobet SA. Disruption of the gene encoding SF-1 alters the distribution of hypothalamic neuronal phenotypes. J Comp Neurol. 2000; 423:579–589. [PubMed: 10880989]

Dornan WA, Akesson TR, Micevych PE. A substance P projection from the VMH to the dorsal midbrain central gray: implication for lordosis. Brain Res Bull. 1990; 25:791–796. [PubMed: 1705159]

Dorner G, Staudt J. Structural changes in the hypothalamic ventromedial nucleus of the male rat, following neonatal castration and androgen treatment. Neuroendocrinology. 1969; 4:278–281. [PubMed: 5796009]

Fahrbach SE, Meisel RL, Pfaff DW. Preoptic implants of estradiol increase wheel running but not the open field activity of female rats. Physiol Behav. 1985; 35:985–992. [PubMed: 4095192]

Farrell MS, Roth BL. Pharmacosynthetics: Reimagining the pharmacogenetic approach. Brain Res. 2013; 1511:6–20. [PubMed: 23063887]

Frank A, Brown LM, Clegg DJ. The role of hypothalamic estrogen receptors in metabolic regulation. Front Neuroendocrinol. 2014:550–557. [PubMed: 24882636]

Ghattas MH, Mehanna ET, Mesbah NM, Abo-Elmatty DM. Association of estrogen receptor alpha gene polymorphisms with metabolic syndrome in Egyptian women. Metabolism. 2013; 62:1437–1442. [PubMed: 23809427]

Griffin GD, Flanagan-Cato LM. Sex differences in the dendritic arbor of hypothalamic ventromedial nucleus neurons. Physiol Behav. 2009; 97:151–156. [PubMed: 19254731]

Hathout GM, Bhidayasiri R. Midbrain ataxia: an introduction to the mesencephalic locomotor region and the pedunculopontine nucleus. AJR Am J Roentgenol. 2005; 184:953–956. [PubMed: 15728623]

Ishii Y, Bouret SG. Embryonic birthdate of hypothalamic leptin-activated neurons in mice. Endocrinology. 2012; 153:3657–3667. [PubMed: 22621961]

Karagiannides I, Bakirtzi K, Kokkotou E, Stavrakis D, Margolis KG, Thomou T, Giorgadze N, Kirkland JL, Pothoulakis C. Role of substance P in the regulation of glucose metabolism via insulin signaling-associated pathways. Endocrinology. 2011a; 152:4571–4580. [PubMed: 22009727]

Karagiannides I, Stavrakis D, Bakirtzi K, Kokkotou E, Pirtskhalava T, Nayeb-Hashemi H, Bowe C, Bugni JM, Nuno M, Lu B, et al. Substance P (SP)-neurokinin-1 receptor (NK-1R) alters adipose tissue responses to high-fat diet and insulin action. Endocrinology. 2011b; 152:2197–2205. [PubMed: 21467195]

Kim KW, Li S, Zhao H, Peng B, Tobet SA, Elmquist JK, Parker KL, Zhao L. CNS-specific ablation of steroidogenic factor 1 results in impaired female reproductive function. Mol Endocrinol. 2010; 24:1240–1250. [PubMed: 20339005]

Kimura S, Hara Y, Pineau T, Fernandez-Salguero P, Fox CH, Ward JM, Gonzalez FJ. The T/ebp null mouse: thyroid-specific enhancer-binding protein is essential for the organogenesis of the thyroid, lung, ventral forebrain, and pituitary. Genes Dev. 1996; 10:60–69. [PubMed: 8557195]

King BM, Frohman LA. Nonirritative lesions of VMH: effects on plasma insulin, obesity, and hyperreactivity. Am J Physiol. 1985; 248:E669–E675. [PubMed: 3890556]

Koch M. Effects of treatment with estradiol and parental experience on the number and distribution of estrogen-binding neurons in the ovariectomized mouse brain. Neuroendocrinology. 1990; 51:505–514. [PubMed: 2112728]

Kopp C, Ressel V, Wigger E, Tobler I. Influence of estrus cycle and ageing on activity patterns in two inbred mouse strains. Behav Brain Res. 2006; 167:165–174. [PubMed: 16214232]

Krashes MJ, Koda S, Ye C, Rogan SC, Adams AC, Cusher DS, Maratos-Flier E, Roth BL, Lowell BB. Rapid, reversible activation of AgRP neurons drives feeding behavior in mice. J Clin Invest. 2011; 121:1424–1428. [PubMed: 21364278]

Kurrasch DM, Cheung CC, Lee FY, Tran PV, Hata K, Ingraham HA. The neonatal ventromedial hypothalamus transcriptome reveals novel markers with spatially distinct patterning. J Neurosci. 2007; 27:13624–13634. [PubMed: 18077674]

Larriva-Sahd J, Rondan-Zarate A, Ramirez-Degollado M. Sexually dimorphic contribution from the fornix to the ventromedial hypothalamic nucleus: a quantitative electron microscopic study. Neurosci Lett. 1995; 200:147–150. [PubMed: 9064598]

Lee H, Kim DW, Remedios R, Anthony TE, Chang A, Madisen L, Zeng H, Anderson DJ. Scalable control of mounting and attack by Esr1+ neurons in the ventromedial hypothalamus. Nature. 2014; 509:627–632. [PubMed: 24739975]

Lin D, Boyle MP, Dollar P, Lee H, Lein ES, Perona P, Anderson DJ. Functional identification of an aggression locus in the mouse hypothalamus. Nature. 2011; 470:221–226. [PubMed: 21307935]

Lubahn DB, Moyer JS, Golding TS, Couse JF, Korach KS, Smithies O. Alteration of reproductive function but not prenatal sexual development after insertional disruption of the mouse estrogen receptor gene. Proc Natl Acad Sci U S A. 1993; 90:11162–11166. [PubMed: 8248223]

MacLusky NJ, McEwen BS. Progestin receptors in rat brain: distribution and properties of cytoplasmic progestin-binding sites. Endocrinology. 1980; 106:192–202. [PubMed: 6243096]

Madeira MD, Ferreira-Silva L, Paula-Barbosa MM. Influence of sex and estrus cycle on the sexual dimorphisms of the hypothalamic ventromedial nucleus: stereological evaluation and Golgi study. J Comp Neurol. 2001; 432:329–345. [PubMed: 11246211]

Marin O, Baker J, Puelles L, Rubenstein JL. Patterning of the basal telencephalon and hypothalamus is essential for guidance of cortical projections. Development. 2002; 129:761–773. [PubMed: 11830575]

Martinez de Morentin PB, Gonzalez-Garcia I, Martins L, Lage R, Fernandez-Mallo D, Martinez-Sanchez N, Ruiz-Pino F, Liu J, Morgan DA, Pinilla L, et al. Estradiol Regulates Brown Adipose Tissue Thermogenesis via Hypothalamic AMPK. Cell Metab. 2014; 20:41–53. [PubMed: 24856932]

Mastronardi C, Smiley GG, Raber J, Kusakabe T, Kawaguchi A, Matagne V, Dietzel A, Heger S, Mungenast AE, Cabrera R, et al. Deletion of the Ttf1 gene in differentiated neurons disrupts female reproduction without impairing basal ganglia function. J Neurosci. 2006; 26:13167–13179. [PubMed: 17182767]

Mermelstein PG. Membrane-localised oestrogen receptor alpha and beta influence neuronal activity through activation of metabotropic glutamate receptors. J Neuroendocrinol. 2009; 21:257–262. [PubMed: 19207809]

Morgan MA, Pfaff DW. Estrogen's effects on activity, anxiety, and fear in two mouse strains. Behav Brain Res. 2002; 132:85–93. [PubMed: 11853861]

Musatov S, Chen W, Pfaff DW, Kaplitt MG, Ogawa S. RNAi-mediated silencing of estrogen receptor {alpha} in the ventromedial nucleus of hypothalamus abolishes female sexual behaviors. Proc Natl Acad Sci U S A. 2006; 103:10456–10460. [PubMed: 16803960]

Musatov S, Chen W, Pfaff DW, Mobbs CV, Yang XJ, Clegg DJ, Kaplitt MG, Ogawa S. Silencing of estrogen receptor alpha in the ventromedial nucleus of hypothalamus leads to metabolic syndrome. Proc Natl Acad Sci U S A. 2007; 104:2501–2506. [PubMed: 17284595]

Narita K, Murata T, Honda K, Nishihara M, Takahashi M, Higuchi T. Subthalamic locomotor region is involved in running activity originating in the rat ventromedial hypothalamus. Behav Brain Res. 2002; 134:275–281. [PubMed: 12191814]

Okura T, Koda M, Ando F, Niino N, Ohta S, Shimokata H. Association of polymorphisms in the estrogen receptor alpha gene with body fat distribution. Int J Obes Relat Metab Disord. 2003; 27:1020–1027. [PubMed: 12917706]

Pfaff D, Keiner M. Atlas of estradiol-concentrating cells in the central nervous system of the female rat. J Comp Neurol. 1973; 151:121–158. [PubMed: 4744471]

Pfaff DW, Sakuma Y. Deficit in the lordosis reflex of female rats caused by lesions in the ventromedial nucleus of the hypothalamus. J Physiol. 1979; 288:203–210. [PubMed: 469716]

Saint-Dizier M, Chastant-Maillard S. Towards an automated detection of oestrus in dairy cattle. Reprod Domest Anim. 2012; 47:1056–1061. [PubMed: 22214367]

Sasaki K, Suzuki M, Mieda M, Tsujino N, Roth B, Sakurai T. Pharmacogenetic modulation of orexin neurons alters sleep/wakefulness states in mice. PLoS One. 2011; 6:e20360. [PubMed: 21647372]

Shimamura K, Rubenstein JL. Inductive interactions direct early regionalization of the mouse forebrain. Development. 1997; 124:2709–2718. [PubMed: 9226442]

Silva BA, Mattucci C, Krzywkowski P, Murana E, Illarionova A, Grinevich V, Canteras NS, Ragozzino D, Gross CT. Independent hypothalamic circuits for social and predator fear. Nat Neurosci. 2013; 16:1731–1733. [PubMed: 24212674]

Skinner RD, Garcia-Rill E. The mesencephalic locomotor region (MLR) in the rat. Brain Res. 1984; 323:385–389. [PubMed: 6525525]

Slonaker JR. The effect of copulation, pregnancy, pseudopregnancy and lactation on the voluntary activity and food consumption of the albino rat. Am J Physiol. 1925; 71

Spiteri T, Ogawa S, Musatov S, Pfaff DW, Agmo A. The role of the estrogen receptor alpha in the medial preoptic area in sexual incentive motivation, proceptivity and receptivity, anxiety, and wheel running in female rats. Behav Brain Res. 2012; 230:11–20. [PubMed: 22321458]

Tran PV, Lee MB, Marin O, Xu B, Jones KR, Reichardt LF, Rubenstein JR, Ingraham HA. Requirement of the orphan nuclear receptor SF-1 in terminal differentiation of ventromedial hypothalamic neurons. Mol Cell Neurosci. 2003; 22:441–453. [PubMed: 12727442]

Xu Y, Nedungadi TP, Zhu L, Sobhani N, Irani BG, Davis KE, Zhang X, Zou F, Gent LM, Hahner LD, et al. Distinct hypothalamic neurons mediate estrogenic effects on energy homeostasis and reproduction. Cell Metab. 2011; 14:453–465. [PubMed: 21982706]

Yang CF, Chiang MC, Gray DC, Prabhakaran M, Alvarado M, Juntti SA, Unger EK, Wells JA, Shah NM. Sexually dimorphic neurons in the ventromedial hypothalamus govern mating in both sexes and aggression in males. Cell. 2013; 153:896–909. [PubMed: 23663785]

Zuloaga DG, Zuloaga KL, Hinds LR, Carbone DL, Handa RJ. Estrogen receptor beta expression in the mouse forebrain: age and sex differences. J Comp Neurol. 2014; 522:358–371. [PubMed: 23818057]

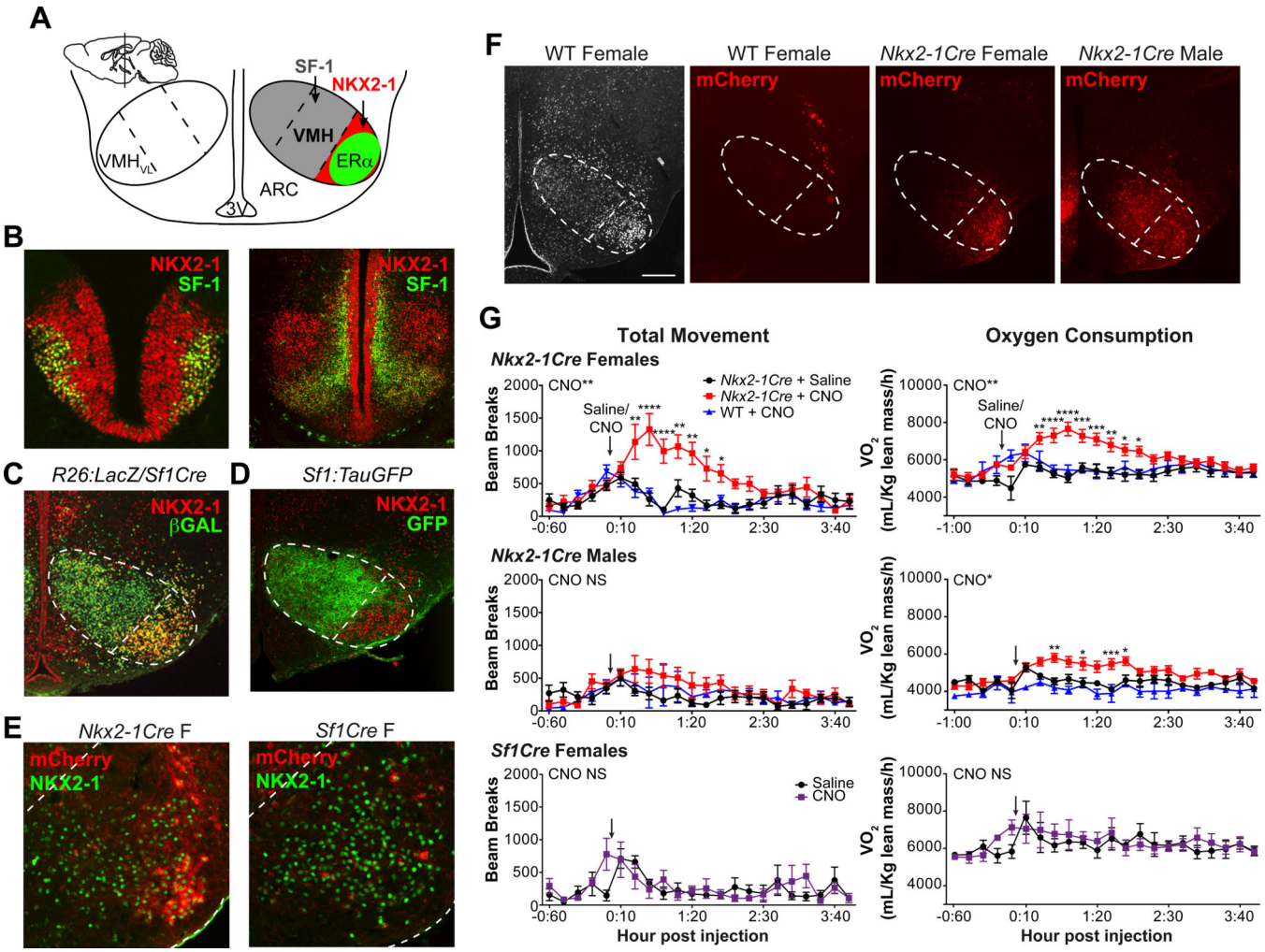

Figure 1. Activating *Nkx2-1* neurons increases movement in female but not male mice

(A) Schematic of the postnatal medial basal hypothalamus (coronal view, sagittal view in inset, modified from Allen Brain Atlas). SF-1$^+$ neurons are found in the dorsomedial and central VMH subregions (grey). NKX2-1$^+$ (red) and ERα$^+$ (green) neurons are confined to the VMH_{VL}.

(B) SF-1 (green) and NKX2-1 (red) immunoreactivity in coronal sections from E11.5 or E13.5 (*Nkx2-1$^{f/f}$* or *Nkx2-1$^{f/+}$/Sf1Cre*) mice.

(C) NKX2-1 (red) and *Cr*--dependent βGAL (green) expression in P0 *Sf1Cre*-expressing mice.

(D) NKX2-1 (red) and GFP (green) immunoreactivity in P0 *Sf1:TauGFP* reporter mice.

(E) mCherry signal (no antibody, red) and NKX2-1 (green) in *Nkx2-1Cre* and *Sf1Cre* female VMH_{VL}.

(F) NKX2-1 immunoreactivity (white) shown for reference and mCherry signal (dsRed immunoreactivity, red) in coronal sections from a wild-type (WT) female, *Nkx2-1Cre* female, and *Nkx2-1Cre* male mice. VMH and VMH_{VL} outlined in dashed lines, DMH = dorsomedial hypothalamus, ARC = arcuate nucleus, 3V = third ventricle, scale bars = 100 μM.

(G) Metabolic chamber analysis of adult *Nkx2-1Cre* females (n = 8), *Nkx2-1Cre* males (n = 7), and *Sf1Cre* females (n=3). Oxygen consumption (VO_2) normalized to grams lean mass and total movement (total beam breaks,×axis) shown 1 h prior to and 4 h following IP injection (arrow) of saline (black circles) or CNO (red squares). Responses to CNO also shown for wild-type female (n = 5) and male (n = 3) littermates (blue triangles). Holm-Sidak multiple comparison tests were used for pairwise comparisons following significant effect of CNO by two-way repeated measures ANOVA (effect of time not shown, effect of CNO in wild-type mice NS). * $p<0.05$, ** $p<0.01$, *** $p<0.001$, **** $p<0.0001$. See also Figures S1 and S2.

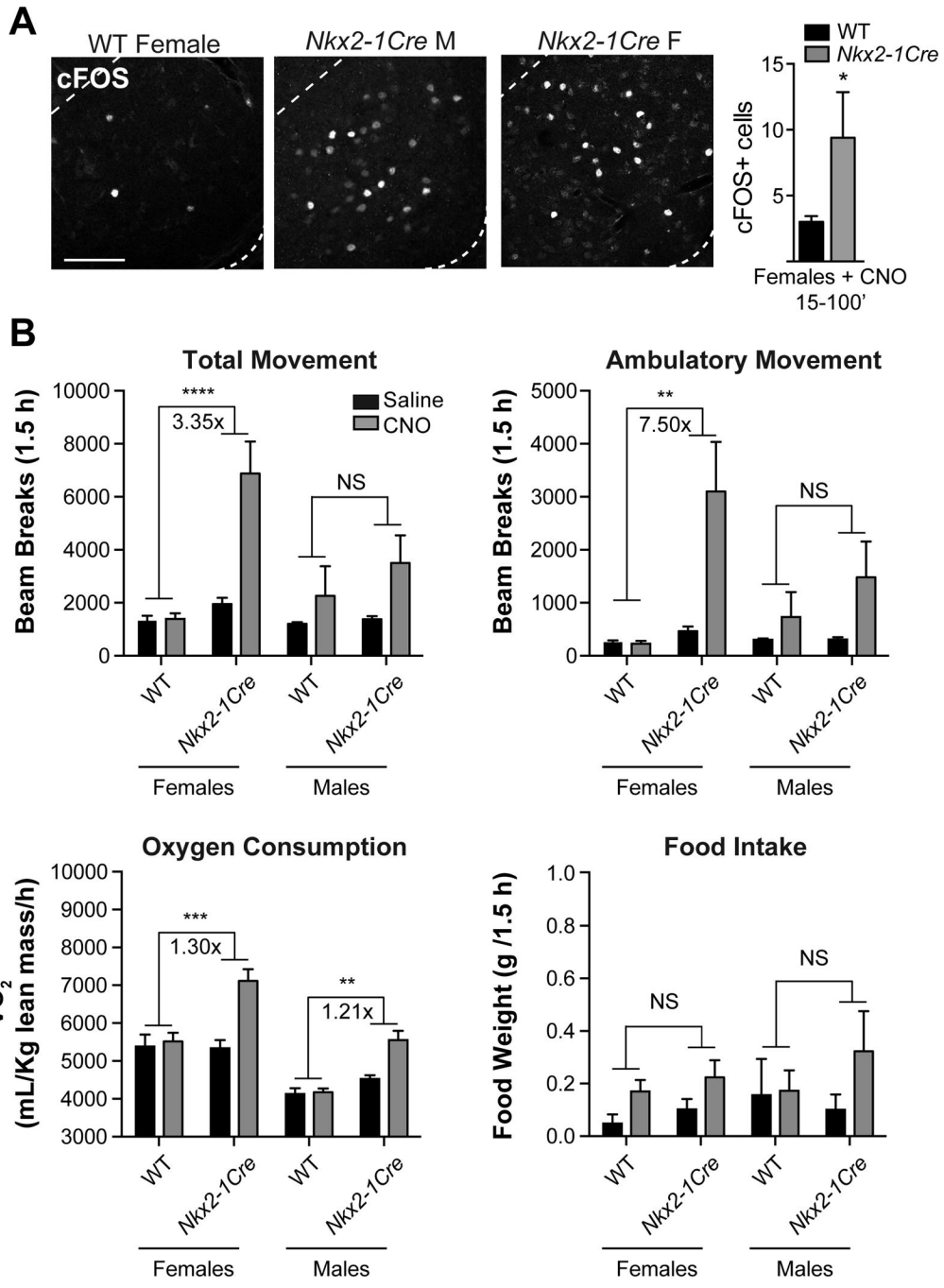

Figure 2. Responses to CNO are greater in *Nkx2-1Cre* mice than wild-type and *Sf1Cre* controls

(A) cFOS immunoreactivity in the VMH_{VL} of *Nkx2-1Cre* female, *Nkx2-1Cre* male, and wild-type female mice 70–75 min after CNO injection. $cFOS^{+}$ cell numbers in one VMH_{VL} from *Nkx2-1Cre* females (n=8) and wild-type females (n=5) analyzed 15–100 minutes after CNO injection, difference significant by two-tailed t-test and by Mann Whitney U test, scale bar = 100 μm.

(B) Average oxygen consumption normalized to lean mass and cumulative total movement, ambulatory movement, and food intake per animal (24–148 minutes, ~1.5 h) after saline

(black) and CNO (grey) in wild-type females (n=5), *Nkx2-1Cre* females (n=8), wild-type males (n = 3), and *Nkx2-1Cre* males (n = 7). Fold-changes comparing the effects of CNO (Nkx2-1Cre(CNO/Saline) / WT (CNO/Saline)) are shown for significant pairwise comparisons. Pairwise comparisons of wild-type and *Nkx2-1Cre* mice treated with CNO were performed using Holm-Sidak multiple comparison tests following significant effects of genotype in a two-way ANOVA ($p<0.05$ for all comparisons shown except food intake), * $p<0.05$, ** $p<0.01$, *** $p<0.001$, **** $p<0.0001$. See also Figure S3.

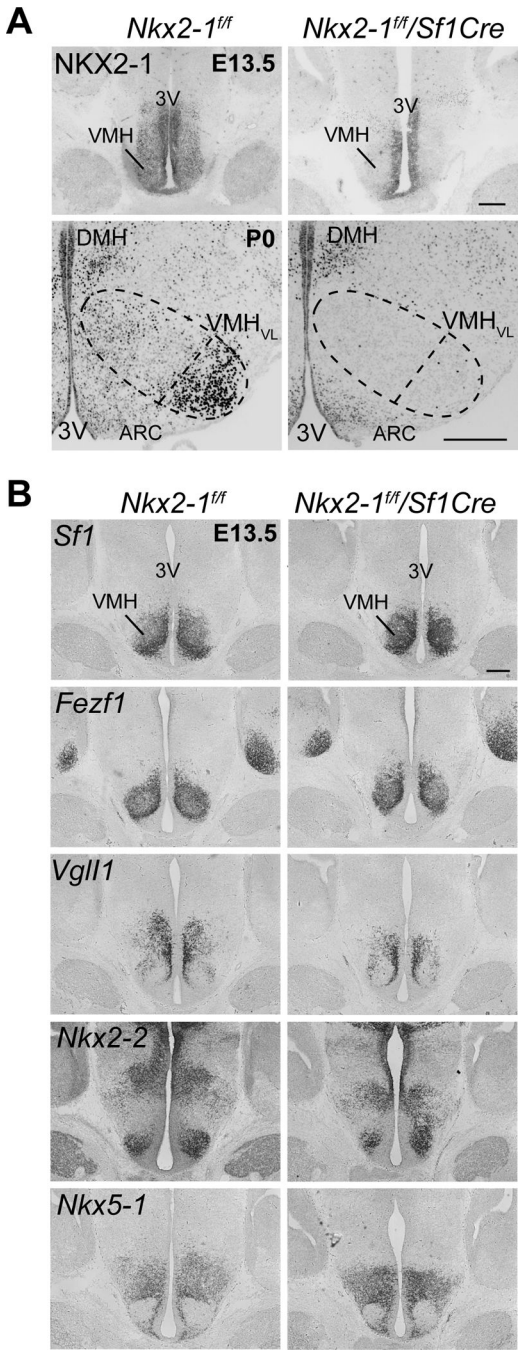

Figure 3. *Nkx2-1* ablation in *Nkx2-1$^{f/f}$/Sf1Cre* mice is specific to the VMH but marker gene expression is largely normal

(A) NKX2-1 immunoreactivity is absent in the VMH of E13.5 or P0 *Nkx2-1$^{f/f}$/Sf1Cre* mice but unchanged in the periventricular area and adjacent nuclei, DMH = dorsomedial hypothalamus, ARC = Arcuate, 3V = third ventricle; scale bars = 500 μm.

(B) RNA in situ hybridization analysis of VMH marker expression in E13.5 *Nkx2-1$^{f/f}$* and *Nkx2-1$^{f/f}$/Sf1Cre* mice. Coronal sections show expression of *Sf1*, *Fezf1* (FEZ family zinc

finger 1), *VglI1* (Vestigial like 1 homolog), *Nkx2-2* (Nk2 homeobox 2), and *Nkx5-1* (Nk5 homeobox 1, also H6 homeobox 3, *Hmx3*). See also Figure S4.

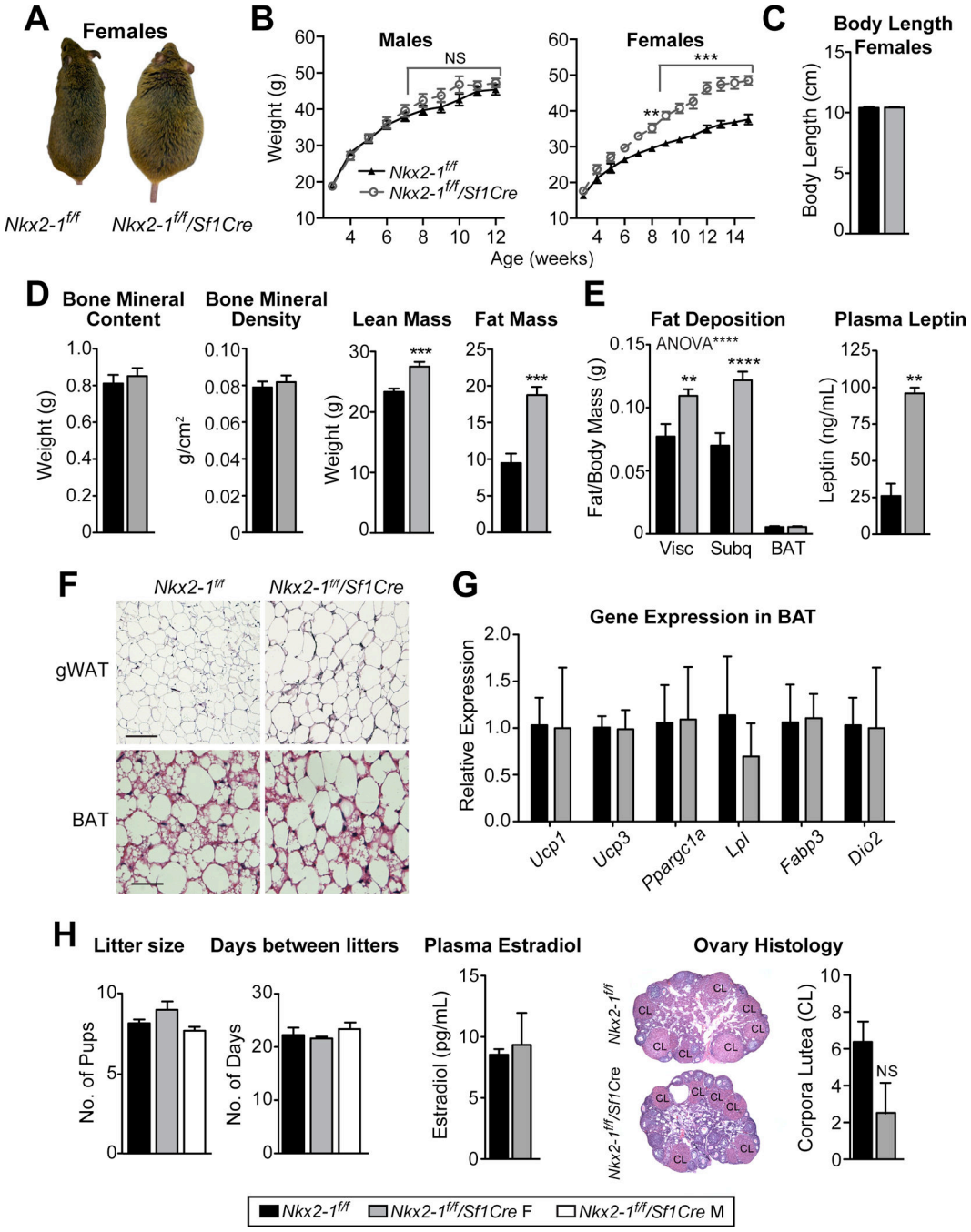

Figure 4. *Nkx2-1* ablation in the VMH results in female specific obesity but does not affect fertility

(A) Photographs of adult *Nkx2-1*$^{f/f}$ and *Nkx2-1*$^{f/f}$*/Sf1Cre* female mice.

(B) Body weight curves from *Nkx2-1f/f/Sf1Cre* (grey open circles, dashed lines) males and females compared to respective control littermates (black triangles, solid lines, n = 8–11/group).

(C, D) Mean body length, lean mass, and fat mass as determined by DEXA for *Nkx2-1*$^{f/f}$*/Sf1Cre* (n = 7) or *Nkx2-1*$^{f/f}$ (n = 8) females at 22 weeks of age.

(E) Mean weights of dissected visceral, subcutaneous and BAT fat depots standardized to total body weight from *Nkx2-1*$^{f/f}$*/Sf1Cre* (n = 5) or *Nkx2-1*$^{f/f}$ (n = 6) females at 22 weeks of age. Plasma leptin (ng/mL) from females analyzed during estrus (n = 2/group).
(F) Representative images of H&E staining of gonadal WAT (gWAT) and BAT in 30 week-old *Nkx2-1*$^{f/f}$*/Sf1Cre* (n = 3) or *Nkx2-1*$^{f/f}$ (n = 2) females.
(G) Transcript expression in BAT from 10 week-old *Nkx2-1*$^{f/f}$*/Sf1Cre* or *Nkx2-1*$^{f/f}$ females (n = 4/group).
(H) Pups per litter produced from mating male and female controls (*Nkx2-1*$^{f/f}$), *Nkx2-1*$^{f/f}$*/Sf1Cre* females with a control males or *Nkx2-1*$^{f/f}$*/Sf1Cre* males with control females (n ≥ 14 litters/group). Plasma estradiol during estrus (pg/mL, n = 2/group), ovarian histology, and number of corpora lutea per section per ovary (n = 4 mice/group). See also Figure S5.

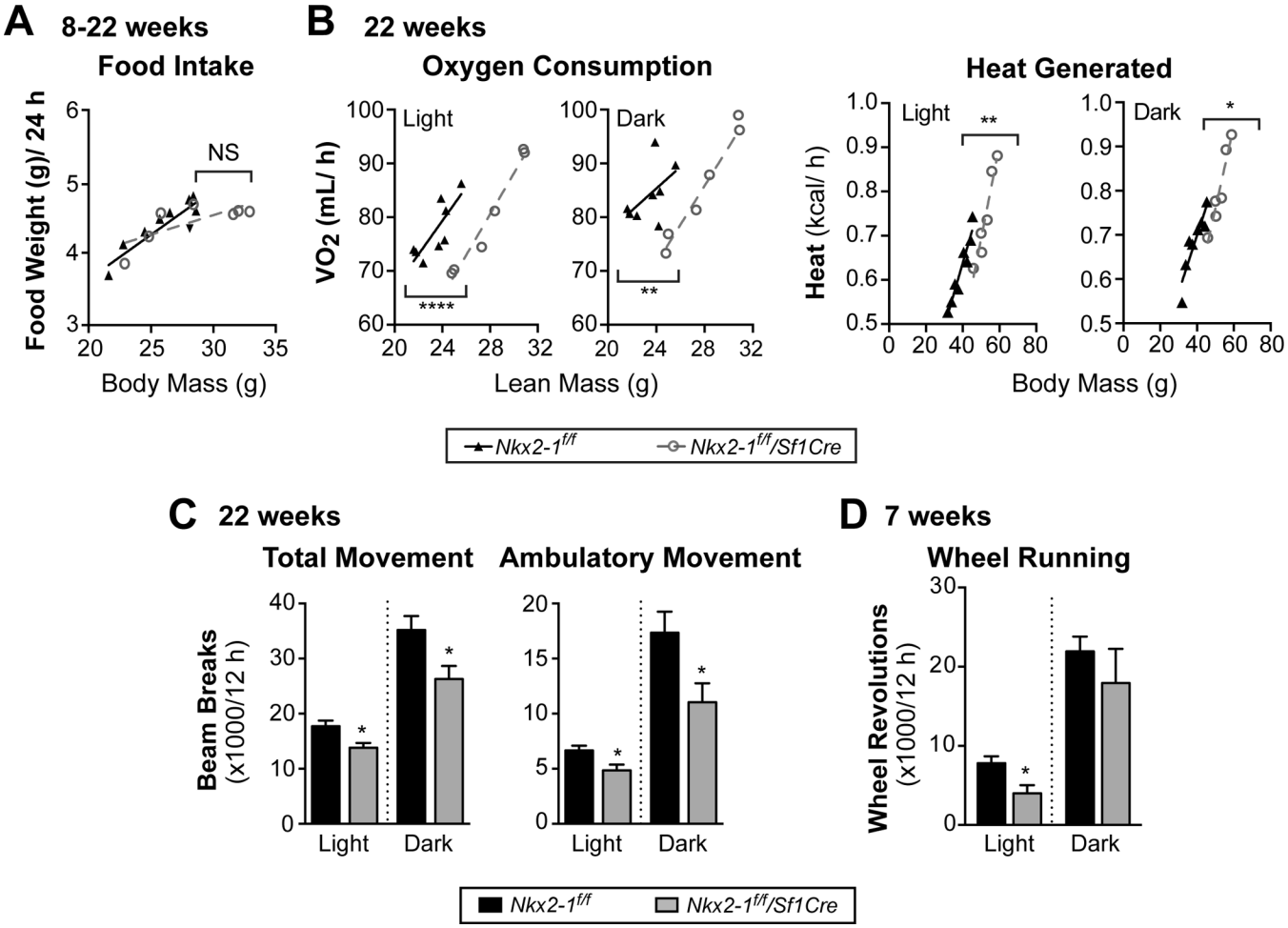

Figure 5. Obese *Nkx2-1* mutant females exhibit reduced physical activity

(A) Daily (24 h) food intake for 8–22 week old singly-housed *Nkx2-1$^{f/f}$/Sf1Cre* (n = 7) or *Nkx2-1$^{f/f}$* female mice (n = 9) over 6 days after 7 days of acclimation, shown relative to total body mass. Food spillage was accounted for in food weight measurements.

(B) VO_2 (mL/h) and heat (kcal/h) per mouse in the light phase (12 h, left panels) or dark phase (12 h, right panels) for 22-week old singly housed *Nkx2-1$^{f/f}$/Sf1Cre* (n = 6) or *Nkx2-1$^{f/f}$* (n = 8) females. Averages (± SE) represent 2 days of acquisition following 2 days of acclimation in metabolic chambers. Linear relationships were analyzed by ANCOVA, achieving better fit with lean mass for VO_2 and body mass for heat generated.

(C) Total movement and Ambulatory movement in 22-week old *Nkx2-1$^{f/f}$/Sf1Cre* (n = 6) or *Nkx2-1$^{f/f}$* (n = 8) mice.

(D) Wheel running in 7-week old *Nkx2-1$^{f/f}$/Sf1Cre* (n = 3) or *Nkx2-1$^{f/f}$* (n = 5) mice over 2 days of acquisition following 9 days of acclimation.

Pairwise comparisons performed with Holm-Sidak multiple comparison tests, * $p<0.05$, ** $p<0.01$, **** $p<0.0001$.

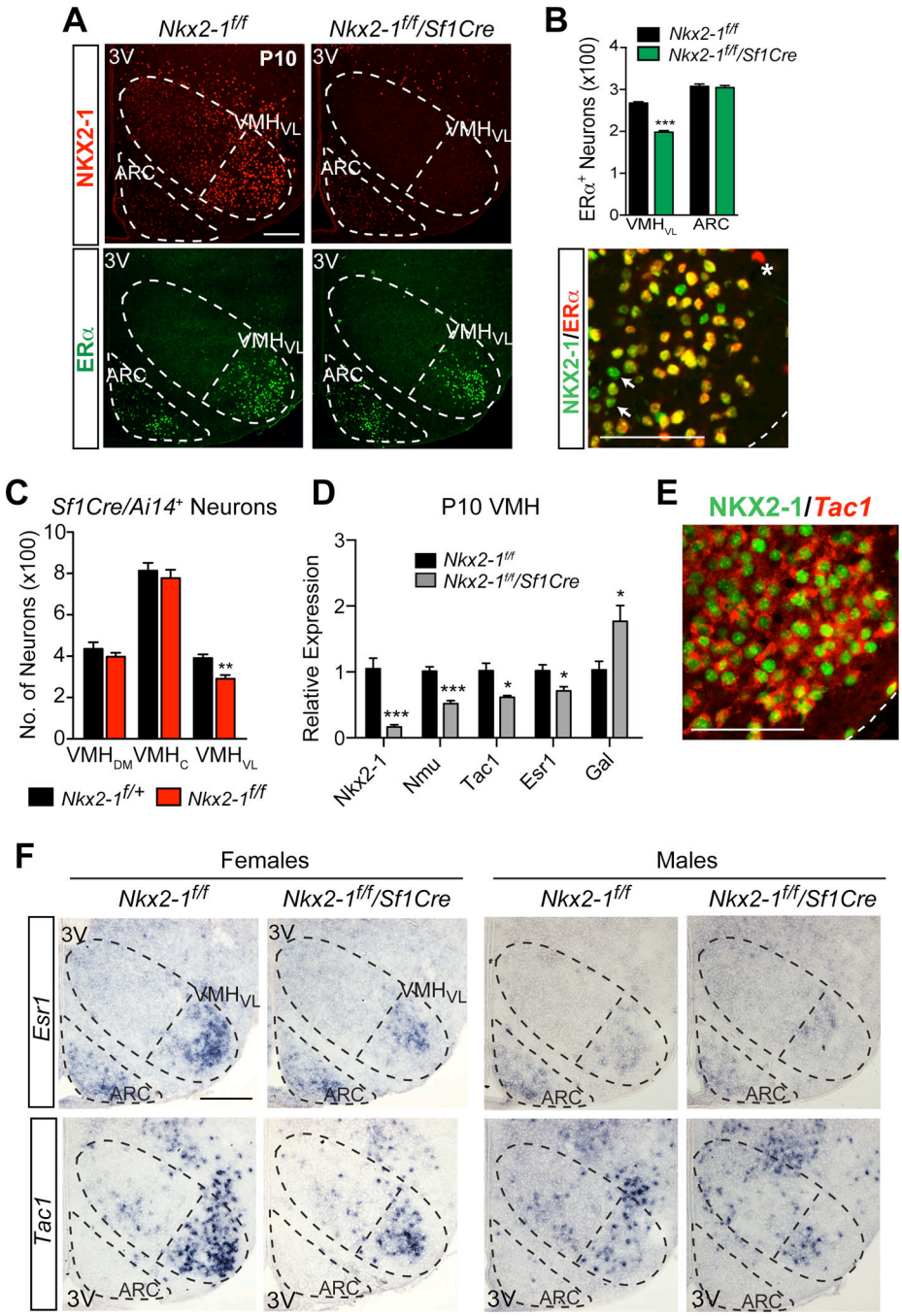

Figure 6. Obesity in *Nkx2-1*$^{f/f}$*/Sf1Cre* females is associated with fewer NKX2-1^{+}, ERα^{+} and *Tac1*$^{+}$ neurons in the VMH$_{VL}$

(A) NKX2-1 (red) and ERα (green) immunoreactivity in the VMH and ARC of P10 *Nkx2-1*$^{f/f}$*/Sf1Cre* and *Nkx2-1*$^{f/f}$ mice. Images show coronal brain sections, VMH, VMH$_{VL}$, and ARC bordered by dashed lines, scale bars = 100 μm, 3V = third ventricle.

(B) Quantification of ERα^{+} nuclei in the VMH$_{VL}$ or ARC from P10 *Nkx2-1*$^{f/f}$*/Sf1Cre* (green) or *Nkx2-1*$^{f/f}$ female mice (black) (n = 2 mice/group, 3 sections/brain). Bottom panel shows double-labeling of NKX2-1 (green) and ERα (red) in the VMH$_{VL}$ of P110 control

females. ERα-negative/NKX2-1-positive (arrows) and ERα-positive/NKX2-1-negative nucleus (asterisk).

(C) Quantification of cells derived from the *Sf1* lineage determined for the ventrolateral (VMH_{VL}), central (VMH_c), and dorsomedial (VMH_{dm}) subregions of *Nkx2-1*$^{f/f}$*/Ai14*$^{f/+}$*/Sf1Cre* mutant (red) and *Nkx2-1*$^{f/+}$*/Ai14*$^{f/+}$*/Sf1Cre* control (black) P10 female mice (n = 5 animals/group, 3 sections/brain).

(D) Relative expression by qPCR of *Nkx2-1*, *Nmu*, *Tac1*, *Esr1*, and *Gal* from microdissected VMH of P10 *Nkx2-1*$^{f/f}$*/Sf1Cre* (grey) or *Nkx2-1*$^{f/f}$ (black) females (n = 3–6/group).

(E) Double-labeling of NKX2-1 immunoreactivity (green, nuclear) and *Tac1* transcripts (red, cytoplasmic) analyzed by confocal microscopy in the VMH_{VL} of P10 wild-type female mice.

(F) Patterns of *Esr1* and *Tac1* transcripts by ISH in *Nkx2-1*$^{f/f}$*/Sf1Cre* or *Nkx2-1*$^{f/f}$ P10 females.

Pairwise comparisons performed with Holm-Sidak multiple comparison tests following two-way ANOVA, * $p<0.05$, ** $p<0.01$, *** $p<0.001$, **** $p<0.0001$. See also Figure S6.

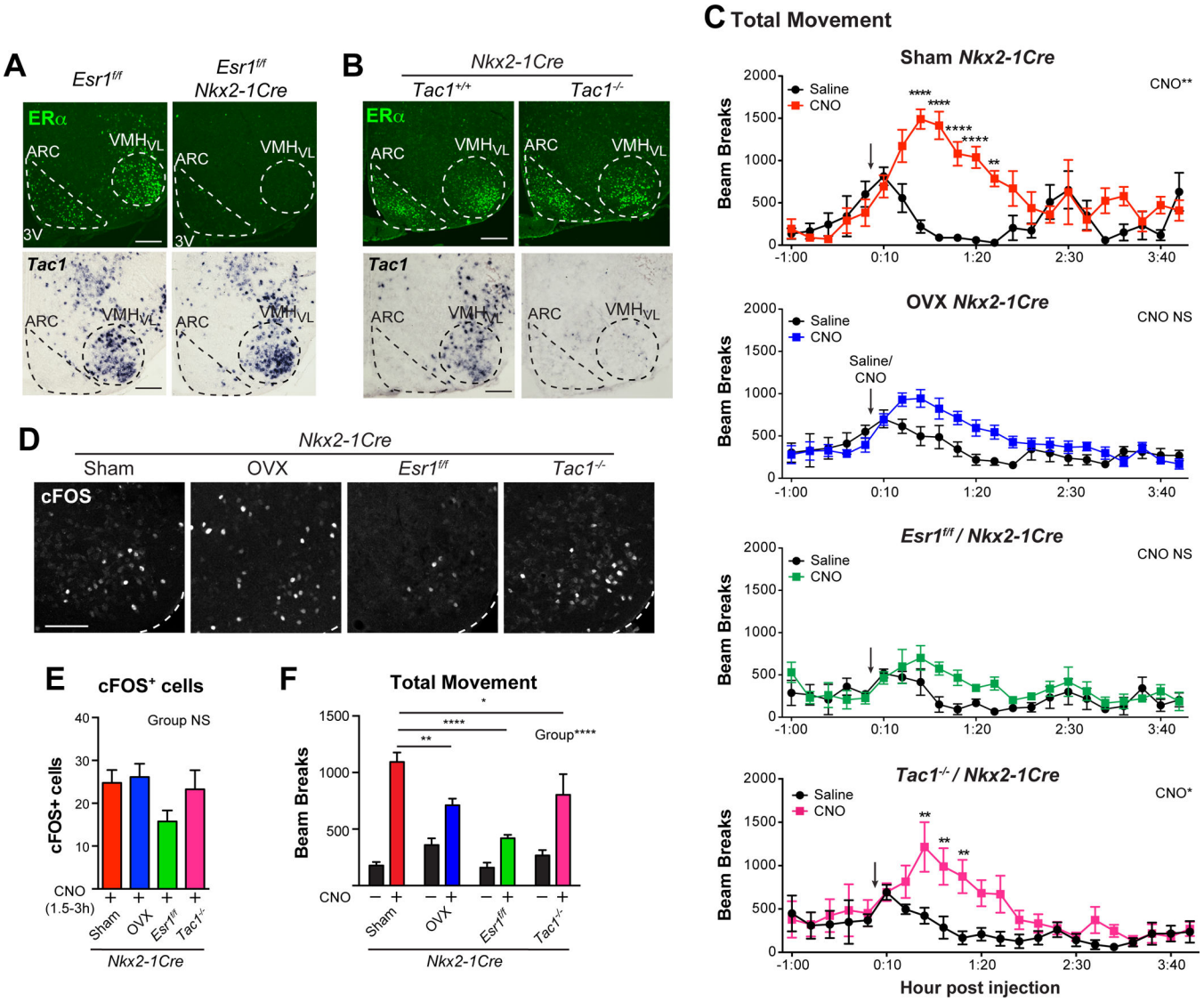

Figure 7. The burst of physical activity after activating *Nkx2-1* VMH_{VL} neurons is dependent on ERα and *Tac1*

(A, B) ERα immunoreactivity or *Tac1* transcript in situ hybridization in *Esr1*$^{f/f}$*/Nkx2-1Cre* or *Tac1*$^{-/-}$ *Nkx2-1Cre* adult female mice (n = 3–4/group). VMH_{VL} and ARC indicated with dashed lines, scale bars = 100 μm.

(C) Total movement (total beam breaks, × axis) in Sham *Nkx2-1Cre* (n = 4), OVX *Nkx2-1Cre* (n=10), *Esr1*$^{f/f}$*/Nkx2-1Cre* (n = 4), and *Tac1*$^{-/-}$*/Nkx2-1Cre* (n = 6) female mice 1 h prior to and 4 h following saline or CNO injection (arrow) in a randomized balanced design.

(D) cFOS immunoreactivity in Sham *Nkx2-1Cre*, OVX *Nkx2-1Cre*, *Esr1*$^{f/f}$*/Nkx2-1Cre*, and *Tac1*$^{-/-}$*/Nkx2-1Cre* female mice analyzed 1.5 h after CNO injection.

(E) Quantification of cFOS^{+} nuclei in all subjects 1.5–3 h after injection, sample sizes as in C.

(F) Average total movement (24–148 minutes) after saline (black bars) and CNO (colored bars), data from C for direct comparison.

Pairwise comparisons performed with Holm-Sidak multiple comparison tests following two-way repeated measures ANOVA, * $p<0.05$, ** $p<0.01$, *** $p<0.001$, **** $p<0.0001$. See also Figure S7.